Energy, Mines and Resources Canada | Énergie, Mines et Ressources Canada

CANMET

Canada Centre for Mineral and Energy Technology | Centre canadien de la technologie des minéraux et de l'énergie

AN EVALUATION OF THE NOTCH TOUGHNESS OF THE HEAT AFFECTED ZONE IN HY AND HSLA SERIES STEELS FOR NAVAL APPLICATIONS

J.T. MCGRATH, J.T.BOWKER, J.A.GIANETTO, R.F.ORR & M.W.LETTS
WELDING SECTION

JANUARY, 1987

PHYSICAL METALLURGY RESEARCH LABORATORY

16 pp
REPORT: PMRL 87-13(TR)

PHYSICAL METALLURGY RESEARCH LABORATORIES
REPORT: PMRL 87-13(TR)

AN EVALUATION OF THE NOTCH TOUGHNESS OF THE HEAT AFFECTED ZONE IN HY AND HSLA SERIES STEELS FOR NAVAL APPLICATIONS

by

J.T.McGrath, J.T. Bowker, J.A. Gianetto, R.F. Orr and M.W. Letts

ABSTRACT

Using the Gleeble 1500 thermal/mechanical simulator the coarse-grain heat-affected zone region (CGHAZ) was simulated in the more conventional HY80, HY100 and Q1N high strength steels for naval application. The notch toughness properties of the CGHAZ of these steels were compared with that of the lower carbon precipitation hardened, HSLA80 steel.

The CGHAZ of the HSLA80 steel had a significantly higher toughness than the HY and Q1N steels in specimens simulated at an energy input of 2 kJ/mm. At an energy input of 4 kJ/mm all of the steels had poor toughness in the CGHAZ. The toughness results are explained on the basis of microstuctural characteristics.

LABORATOIRES DE RECHERCHE EN METALLURGIE PHYSIQUE

RAPPORT: PMRL 87-13(TR)

ETUDE DE LA RESILIENCE DE LA ZONE ATTAQUEE PAR LA CHALEUR D'ACIERS DE QUALITE HY ET HSLA DESTINES AUX APPLICATIONS NAVALES

par

J.T. McGRATH, J.T. BOWKER, J.A. GIANETTO, R.F. ORR et M.W. LETTS

RESUME

On a employé le simulateur thermomécanique Gleebe 1500 pour simuler les zones thermiquement affectées à grains grossiers (ZTAGG) d'aciers hautement résistants de qualité HY80, HY100 et QIN destinés à des applications navales. Les propriétés de résilience de la ZTAGG de ces aciers ont été comparées à celles d'un acier durci par précipitation, de qualité HSLA 80 à faible teneur en carbone.

La ZTAGG de l'acier de qualité HSLA 80 a une résistance plus élevée que celle des aciers expérimentaux HY et QIN simulés en fonction de l'apport de chaleur 2 kJ/mm. Cependant, tous les aciers ont démontré une faible résilience au niveau de la ZTAGG avec un apport de chaleur de 4 kJ/mm. Tous les résultats d'essais des études sur la résilience sont expliqués suivant des caractéristiques microstructurales.

INTRODUCTION

This report provides a comparison of the heat-affected-zone (HAZ) microstructure and notch toughness properties of the high strength HY series and HSLA80 steels being considered for application in naval ships and submarines. Simulated coarse-grain heat-affected zone structures were produced as a function of weld energy input for the study. The targeted notch toughness properties for the HAZ were obtained from consideration of present military standards for submarine fabrication. Although the military standard for submarine construction MIL-STD-1688(SH)(1) requires impact energies for weld metals of 27J at -50°C and 81J at -18°C a more stringent requirement is needed from a consumable qualification standpoint. In this regard impact energies of 47J at -50°C and 81J at -18°C are specified in weld metal qualification standard MIL-E-23765/2C (2). At present military standards do not require Charpy impact testing of the HAZ region and specific requirements for HAZ notch toughness properties are unresolved. Therefore, the targeted values for the purpose of comparison and evaluation of the HAZ toughness were designated as 47J at -50°C and 81J at -18°C.

EXPERIMENTAL PROCEDURE

MATERIALS

The evaluation of heat-affected zone microstructure and mechanical properties was performed on a range of high strength steels for naval application. The composition of these steels which included HY80, Q1N, HY100 and HSLA80, are listed in Table 1. The HY series and Q1N steels are representative of the high carbon, hardenable quenched and tempered steels with the Q1N steel having the lowest sulphur content. The HSLA80 is a lower carbon steel which gains its properties from the formation of copper precipitate particles after heat treatment.

SIMULATION OF THE HAZ

The Gleeble 1500 thermal/mechanical simulator was used to simulate the coarse-grained heat-affected zone (CGHAZ) in the high strength steels. A peak temperature of 1350°C and cooling times of 11.5 and 45 seconds represented the cooling rates for welding of a 25 mm thick plate at energy inputs of 2 and 4 kJ/mm, respectively.

The Gleeble specimens, 10 mm x 10 mm x 75 mm, were machined from the base materials with the long axis transverse to the plate rolling direction. The simulated CGHAZ was contained in approximately 5 mm of the central portion of the specimen. Following the weld thermal cycling, specimens were notched through-thickness for Charpy-V notch toughness testing. Charpy transition curves were obtained for all HAZ simulated structures.

Optical metallography was performed to characterize the microstructures for each test condition. Scanning electron microscopy was employed to examine the fractured surfaces of selected Charpy specimens.

RESULTS

HAZ NOTCH TOUGHNESS PROPERTIES

The Charpy impact transition curves of the Gleeble simulated CGHAZ for the various steel compositions are shown in Figs. 1, 2 and 3 as a function of energy input. Only the HSLA80 steel simulated at the energy input of 2 kJ/mm met the targeted HAZ notch toughness of 47J at -50°C and 81J at -18°C. There was no change in notch toughness properties with energy input for either the HY80 or the HY100 steels. The CGHAZ toughness for the Q1N steel also did not vary significantly with energy input, but the overall level of toughness was higher than either the HY80 or HY100 steels.

The CGHAZ of the HSLA80 steel simulated at the energy input of 2 kJ/mm had considerably higher toughness compared with that of the HY series and Q1N steels over the full test temperature range (Fig. 3). For specimens subjected to the 4 kJ/mm simulation, the notch toughness decreased sharply at temperatures <10°C.

HAZ MICROSTRUCTURE

A totally martensitic microstructure in the CGHAZ was observed at both the 2 and 4 kJ/mm energy input simulations for the HY80, HY100 and Q1N steels. This structure is shown typically in Fig. 4. The microhardness readings for these simulated HAZ specimens were in excess of 400 DPH as indicated in Table 2. SEM observations of fractured surfaces (Fig. 5) and optical metallography revealed the presence of intercrystalline facets caused by liquation cracking in the simulated HY80, HY100 and Q1N specimens. However Q1N contained a significantly lower proportion of intercrystalline discontinuities compared with HY80 and HY100.

The microstructure of the CGHAZ of the HSLA80 steel was composed predominantly of low carbon martensite with some bainitic regions after simulation at 2 kJ/mm. Using the terminology of Torronen (3) the martensitic structure in Fig. 6a consisted of elongated packets or laths which formed in bundles within prior austenite grains. Although transmission electron microscopy was not employed to measure the orientation relationship between adjacent packets it was assumed, based upon other studies of low carbon martensite (3,4) and from SEM observations of fractured surfaces, that the boundaries between packets were mainly high angled.

The CGHAZ of the HSLA80 steel contained entirely coarse bainite after simulation at 4 kJ/mm. This bainitic structure, shown in Fig. 6b, consisted of parallel bainitic ferrite laths separated by elongated martensite-austenite (MA) regions. The misorientations between adjacent laths are assumed to be low angle boundaries from fractographic evidence and electron diffraction results in other investigations of bainitic microstructure (4). For the bainitic microstructure, a packet consists of a group of parallel laths. As shown

in Fig. 6b a prior austenite grain may contain one or as many as three packets.

The SEM observations of the fractured surfaces of the HSLA80 simulated specimens provide evidence of the unit fracture length or cleavage facet size associated with low temperature fracture as well as the relative misorientation between packets for both the martensitic and bainitic microstructures. The cleavage facets for the 2 kJ/mm simulated specimens, shown in Fig. 7a, were elongated and ranged in width from 5 to 10 μm. These features compare with the shape and dimensions of the individual martensitic packets shown in Fig. 6a. The much larger cleavage facets (40 to 80 μm) observed in the fractured 4 kJ/mm simulated specimens, (Fig. 7b) related to the bainitic packet size shown in Fig. 6b.

DISCUSSION

The notch toughness properties of the CGHAZ of the various high strength steels can be explained on the basis of microstructural characteristics. For the higher carbon, hardenable quenched and tempered HY series steels, it was revealed from previous work (6,7) that the liquation of sulphide inclusions in the CGHAZ during welding was a significant factor in lowering the notch toughness properties of this region. The sulphides which melt in the HAZ near the fusion line during welding penetrate and weaken austenitic grain boundaries by forming sulphide films during cooling (8,9). The tensile stresses generated in the welding cycle can produce discontinuities or microcracking along grain boundaries in the CGHAZ. Liquation embrittlement in the HAZ of HY80 weldments has been shown to increase with increasing carbon content and to decrease with increasing Mn/S ratio (10). The study of Q1N steel with a lower sulphur (0.005%) and higher Mn/S ratio (58/1was intended to reduce liquation embrittlement in the CGHAZ and hence to significantly improve the notch toughness properties. The notch toughness results in Fig.1 indicate an improvement in toughness in the Q1N Gleeble simulated specimens compared to the HY80 steel but the notch toughness

properties of the CGHAZ were still below the targeted values despite the reduction in liquation embrittlement. For the HY100 steel, the tendency for liquation embrittlement in the CGHAZ had been reduced as a result of a higher Mn/S ratio (see Table 1). Therefore, one can conclude for the HY and Q1N steels, that the presence of high carbon untempered martensite in the CGHAZ makes the most significant contribution to the overall low notch toughness properties.

The excellent notch toughness properties of the CGHAZ of the HSLA80 steel subjected to Gleeble simulation of 2 kJ/mm, particularly at low temperatures, can be attributed to the characteristics of the low carbon martensitic structure. It was determined from SEM examination of the fractured surface that the cleavage facet size corresponded to the dimensions of the individual martensite packets i.e., 5 to 10 μm. This indicates that when cleavage fracture initiates within an individual packet it must reinitiate at each high angle packet boundary in order to continue propagation through the CGHAZ. The finer the packet size, the higher the resistance to cleavage fracture. The coarse, bainitic structure developed in the CGHAZ of the HSLA80 steel subjected to the 4 kJ/mm simulation was responsible for the poor low temperature notch toughness properties. The large cleavage facets observed in the fractured specimens are formed when a crack initiates in a packet and propagates with little resistance across the low angle boundaries which separate the parallel laths within a packet. Reinitiation takes place at the high angle packet boundaries.

CONCLUSIONS

1. In the energy input range of 2 to 4kJ/mm the Gleeble simulated CGHAZ of the HY80, HY100 and Q1N high strength steels had poor notch toughness properties which were significantly below the targeted levels of 47 J at -50°C and 81 J at -18°C.

2. Although the formation of liquation cracking in the CGHAZ was reduced as the sulphur level was lowered in the HY and Q1N steels, the overall low toughness properties of the CGHAZ were attributed primarily to the formation of hard, untempered martensite.

3. The HSLA80 steel subjected to Gleeble simulation at 2 kJ/mm exhibited excellent notch toughness in the CGHAZ exceeding the targeted values. The low carbon martensite microstructure conferred effective fracture resistence.

4. Under high energy input conditions (4 kJ/mm) the HSLA80 steel had poor HAZ toughness. The coarse upper bainite microstructure was responsible for the low toughness of the CGHAZ.

REFERENCES

1. U.S. Dept. of Defence, Military Specification MIL-STD-1688(SH), 1981.

2. U.S. Dept. of Defence, Military Specification MIL-E- 23765/2C, 1983.

3. K. Torronen; Microstructural Parameters and Yielding in Quenched and Tempered Cr-Mo-V Pressure Vessel Steel, Research Centre of Finland, 1979, Publ. 22.

4. M.J. Roberts; Met. Trans., 1970, Vol. 1, pp. 3287-3294.

5. F.B. Pickering; Transformation and Hardenability in Steels, Climax Molybdenum Co. of Michigan Symp., 1967, pp. 109-129.

6. K. Romhanyi, M.R. Krishnadev, R.D. McDonald, J.T. Bowker and J.T. McGrath; Microstructural Science, 1985, Vol. 14, pp. 115-126.

7 J.T. McGrath, J.A. Gianetto, R.F. Orr and M.W. Letts; Can. Met. Quarterly, in press, 1987.

8. R.H. Phillips and M.F. Jordan; Metals Tech., 1976, Vol. 3, pp. 571-579.

9. R.H. Phillips and M.F. Jordan; Metals Tech., 1977, Vol. 4, pp. 396-405.

10. C.F. Meitzner and R.D. Stout; Weld, J., 1966, Vol. 45, pp. 393-S-400-S.

Table 1 - Chemical composition of high-strength steels

Base Metal	Element wt %										
	C	Mn	Si	S	P	Ni	Cr	Mo	Cu	V	Nb
HY80	0.17	0.30	0.19	0.014	0.007	2.59	1.53	0.42	0.03	0.010	0.005
Q1N	0.17	0.29	0.25	0.005	0.010	2.66	1.39	0.36	0.07	0.010	0.015
HY100	0.17	0.33	0.23	0.008	0.010	2.62	1.52	0.48	0.04	0.005	0.012
HSLA80	0.06	0.50	0.27	0.004	0.007	0.92	0.66	0.25	1.02	0.005	0.044

Table 2 - Microhardness of as-received and simulated CGHAZ in the high-strength steels

Microhardness, DPH			
Base metal	As-received	Simulated CGHAZ	
		2 kJ/mm	4kJ/mm
HY80	217	410	409
Q1N	241	429	419
HY100	287	452	450
HSLA80	246	306	242

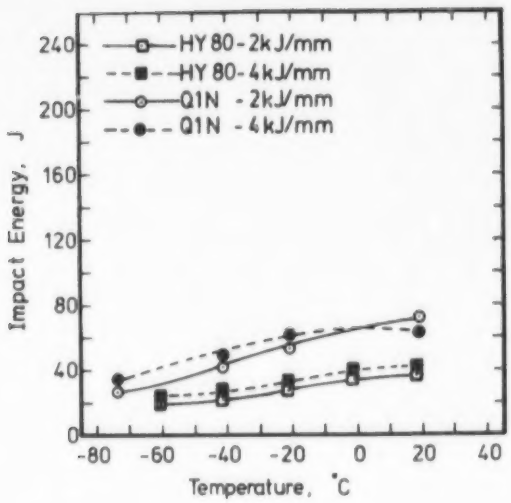

Fig. 1. Charpy transition curves of simulated CGHAZ in HY80 and Q1N steels (neg 15284)

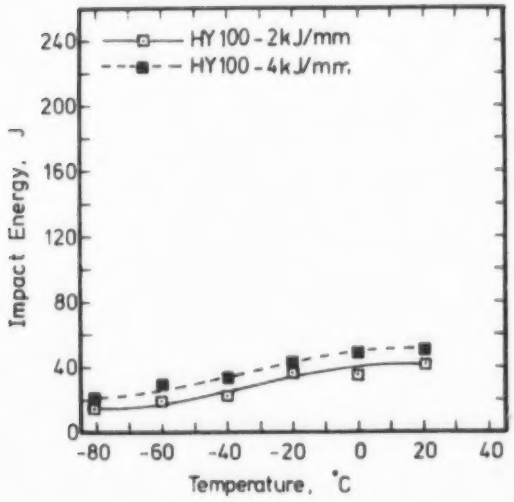

Fig. 2. Charpy transition curves of simulated CGHAZ in HY100 steel (neg 15285)

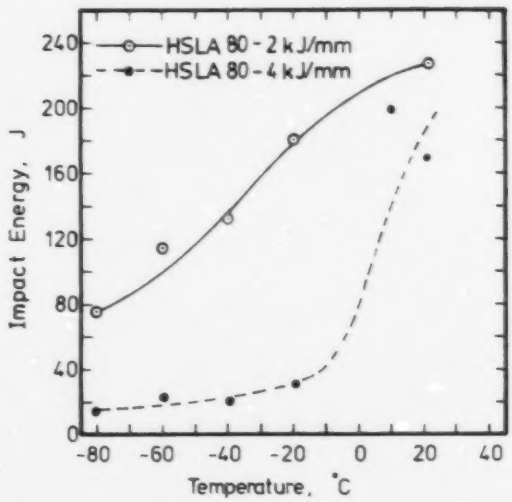

Fig. 3. Charpy transition curves of simulated CGHAZ in HSLA80 steel (neg 15286)

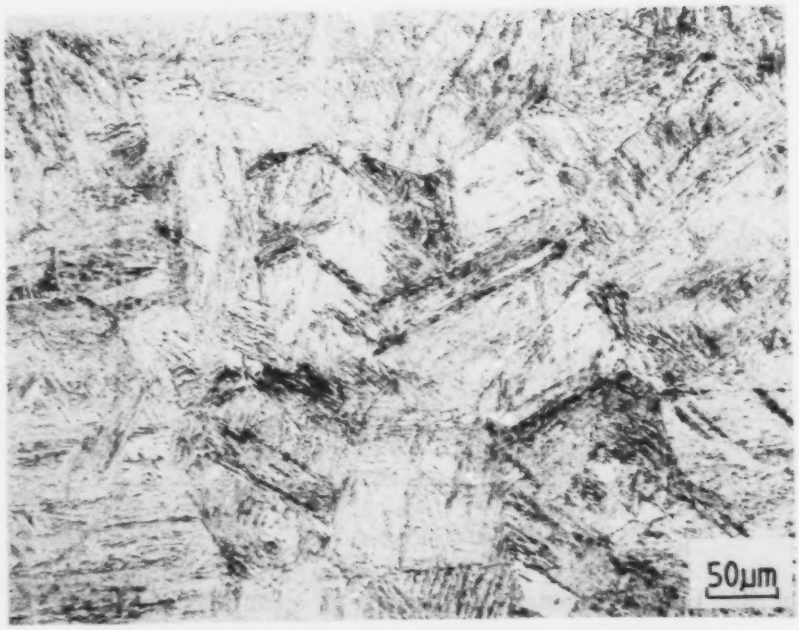

Fig. 4. Microstructure of simulated CGHAZ in HY80 cycled at kJ/mm.(neg 14661)

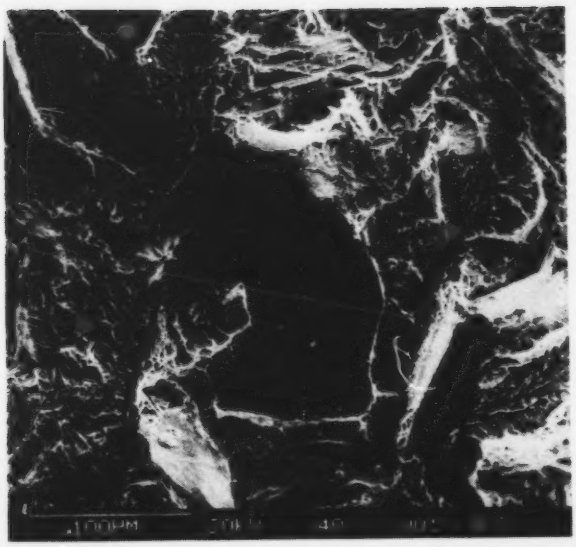

Fig. 5. SEM fractograph showing intercrystalline facets on fracture surface of HY80 steel.

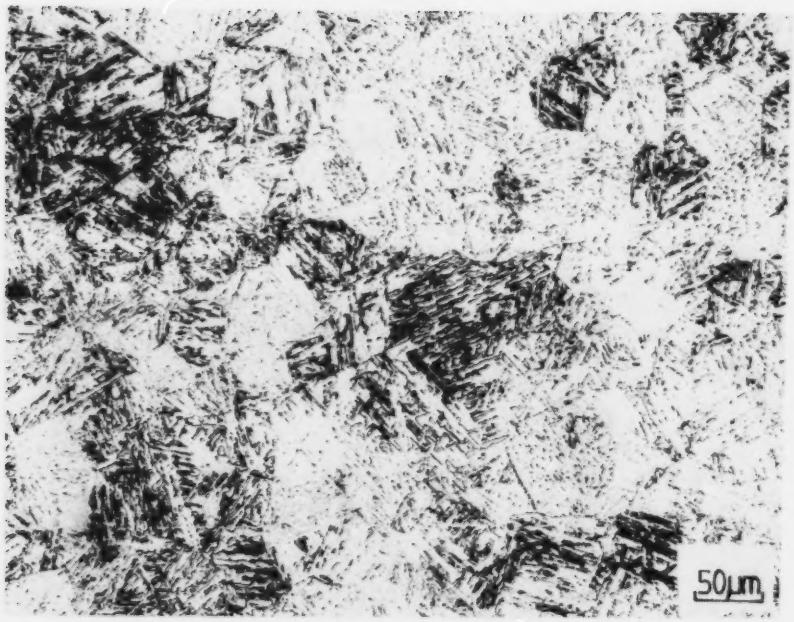

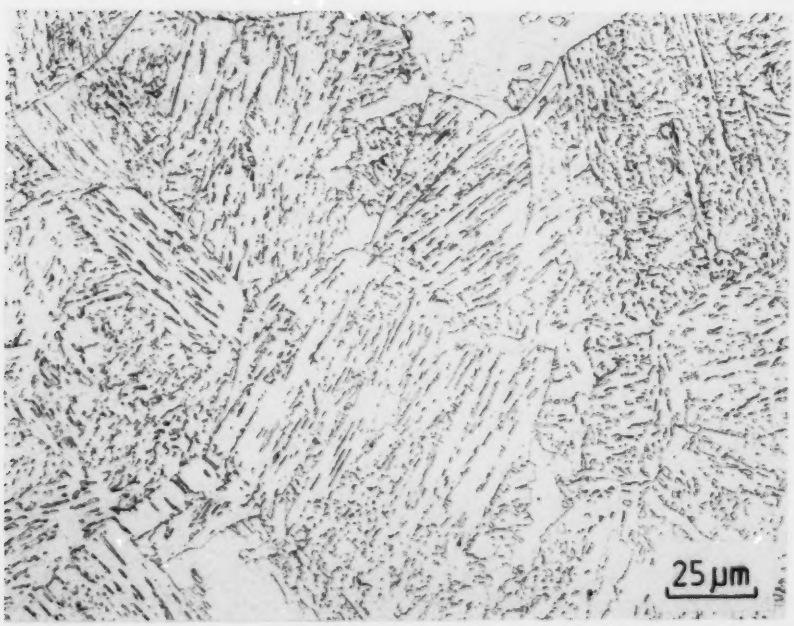

Fig. 6. Optical micrographs of simulated CGHAZ of HSLA80 2 kJ/mm (b) 4 kJ/mm. (neg 15376, 15375)

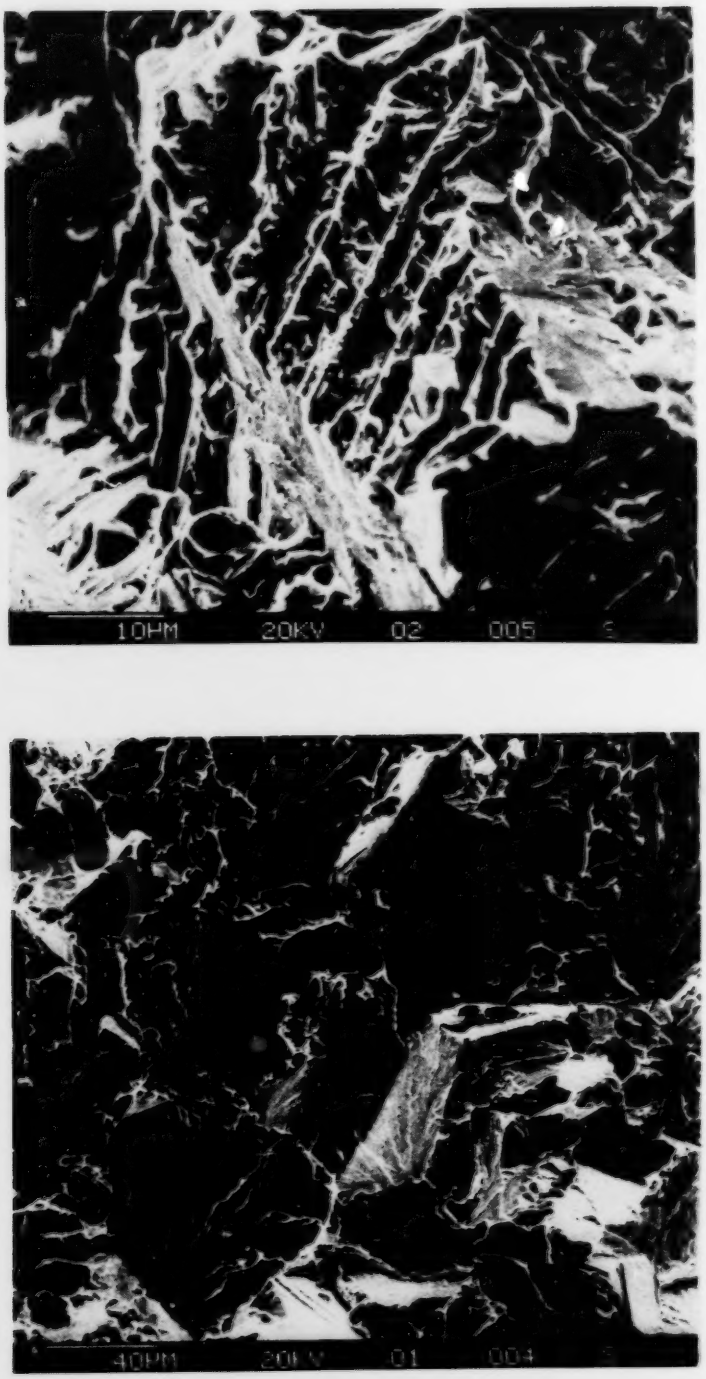

Fig. 7. SEM fractographs showing cleavage facets for simulated CGHAZ of HSLA80 steel. (a) 2 kJ/mm (b) 4 kJ/mm.